Geological Quarterly, 2005, **49** (2): 173–184

Stable isotopic and mineralogical investigations of an arid Quaternary lacustrine palaeoenvironment, Western Qaidam, China

Ana-Voica BOJAR, Andrea RIESER, Franz NEUBAUER, Hans-Peter BOJAR, Johann GENSER, Yongjiang LIU and Xiao-Hong GE

Bojar A.-V., Rieser A., Neubauer F., Bojar H.-P., Genser J., Liu Y. and Ge X.-H. (2005) — Stable isotopic and mineralogical investigations of an arid Quaternary lacustrine palaeoenvironment, Western Qaidam, China. Geol. Quart., **49** (2): 173–184. Warszawa.

Stable isotope analyses on carbonates from lake evaporites collected from the non-marine western Qaidam basin yield a positive excursion from Pliocene to Quaternary times. At Dafeng Shan, the Quaternary sequences are composed of alternating layers of celestine/dolomite and aragonite/calcite/barite with distinct isotopic compositions. The sequence described at Dafeng Shan formed in a low energy, hypersaline lacustrine environment as indicated by the microstructures and evaporitic minerals as well as by the absence of lithoclasts. The peloids, ooids and oncoids described are related to microbial activities in saline lake. The oxygen isotopic composition of the carbonates vary between +34.4 and +39.8‰ (SMOW), representing the heaviest values measured until now. The ^{18}O and the ^{34}S isotopic composition of the celestine range between 20.1 to 22.3‰ (SMOW) and +19 to +22‰ (CDT) respectively, suggesting sulfur recycling via sulfide oxidation. The carbon isotopic compositions of the carbonates show a large negative excursion of up to –30‰. The microstructures, mineralogy and isotopic compositions as well as the geological context suggest oxidation of methane from a deep source.

Ana-Voica Bojar, Institute of Earth Science, Geology and Paleontology, Karl-Franzens University, A-8010 Graz, Austria, e-mail: ana-voica.bojar@uni-graz.at; Andrea Rieser, Franz Neubauer and Johann Genser, Department of Geography, Geology and Mineralogy, Divison General Geology and Geodynamics, Paris-Lodron University, A-5020 Salzburg, Austria; Hans-Peter Bojar, Department of Mineralogy, Landesmuseum Joanneum, A-8010 Graz, Austria; Yongjiang Liu and Xiao-Hong Ge, Faculty of Earth Sciences, Jilin University, 130061 Changchun, China (received: November 8, 2004; accepted: April 11, 2005).

Key words: Qaidam, Quaternary, stable isotopes, celestine, carbonates, hypersaline lacustrine environment.

INTRODUCTION

The Himalayas, the Tibetan plateau and the adjacent mountains to the north, are the largest present-day topographic features resulting from continent–continent collision (e.g., Molnar and Tapponnier, 1975; Allégre *et al*., 1984; Yin and Nie, 1996; Hodges, 2000). The average elevation of the region reaches 4000–5000 metres. The progressive north-south shortening, due to collision, achieves *ca*. 1400 km (e.g., Zhou and Graham, 1996; Replumaz and Tapponnier, 2003). The Neohimalayan tectonic phase started during the early Miocene (e.g., Hodges, 2000) and has been followed by accelerated denudation during the past few million years. Accelerated denudation may have been triggered by either tectonic activity, as suggested by recent seismic movements within the Himalayan Metamorphic Belt, or by enhanced erosion, possibly related to global climate changes (An *et al*., 2001; Kayal, 2001; Peizhen *et al*., 2001; Bojar *et al*., 2005).

The onset of the Indian and East Asian monsoon, as well as enhanced aridity in the Central Asia, occurred about 8 Ma ago, concomitant with a period of significant increase in the altitude of the Tibetan plateau and with Northern Hemisphere glaciation (Harrison *et al*., 1992; Prell and Kutzbach, 1992; Molnar *et al*., 1993; Ramstein *et al*., 1997; Lehmkuhl and Haselein, 2000; Peizhen *et al*., 2001; Zhisheng *et al*., 2001; Guo *et al*., 2002). Later intensifications of the East Asian monsoon at 3.6 and 2.6 Ma are also related to periods of rapid uplift of the northwestern part of the Tibetan plateau (Qiang *et al*., 2001; Spicer *et al*., 2003).

The Qaidam basin is located at the northern edge of the Tibetan plateau. The thick Pliocene-Quaternary deposits were influenced by tectonic processes related to uplift of the Tibetan plateau, as well as by climatic changes related to plateau growth (Harrison *et al*., 1992; Murphy *et al*., 1997; Meyer *et*

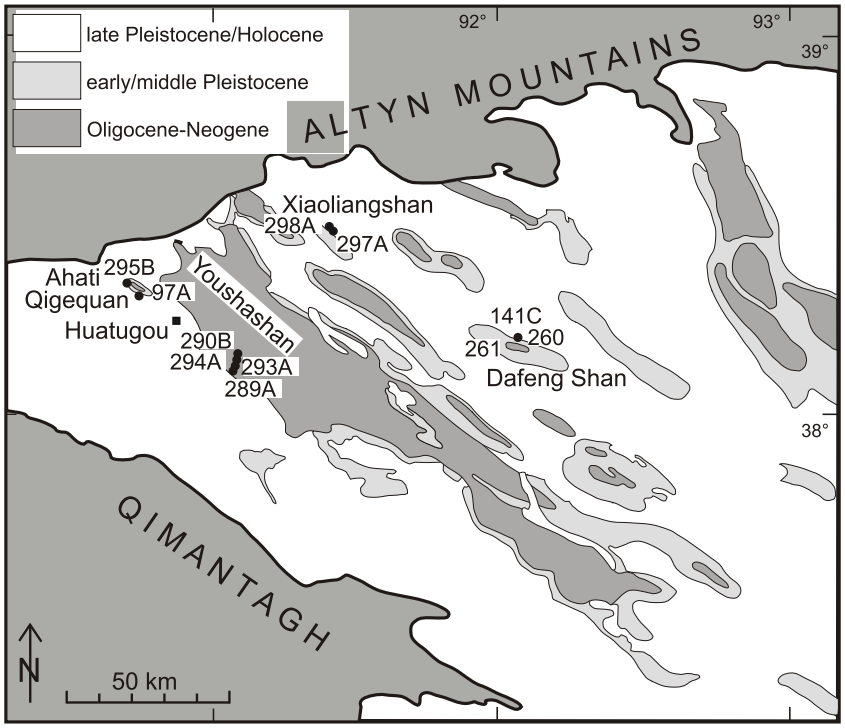

Fig. 1. Simplified map of the western part of the Qaidam basin and location of investigated samples

al., 1998). Different approaches have been used in order to reconstruct Cenozoic environmental changes from the sedimentary record of the basin. These include pollen analysis, stratigraphy, dating of evaporite deposits, stable isotopes of fluid inclusions in evaporites, and the areal extent of salt lakes (Chen and Bowler, 1986; Phillips *et al*., 1993; Yang *et al*., 1995; Liu *et al*., 1998; Wang *et al*., 1999).

In this study we have reconstructed Pliocene and Quaternary lacustrine palaeoenvironment by examining the mineralogy, fabrics and geochemistry of climate-sensitive rocks, in this case the carbonates and sulphates from the western part of the Qaidam basin (Fig. 1).

GEOLOGICAL FRAMEWORK AND PLIOCENE TO QUATERNARY CLIMATE CHANGES IN THE QAIDAM BASIN

The *ca*. 120 000 km^2 large, rhomb-shaped Qaidam basin, containing unusually thick (3–17 km) Mesozoic to Cenozoic sedimentary sequences, is surrounded by the Kunlun/Qimantagh, Qilian and Altyn mountain ranges. The mean surface elevation of the basin floor is ~2700 m, whereas the surrounding mountains reach elevations of over 5000 m. The latest interpretations consider the formation of the Qaidam basin as a response to oblique compression between the left lateral Altyn and Central Kunlun faults (Métivier *et al*., 1998; Meyer *et al*., 1998). The basin stratigraphy is well constrained by ostracods, spores, pollen, magnetostratigraphy and seismic stratigraphy (Sun *et al*., 1999; Wang *et al*., 1999; Xia *et al*., 2001 and references therein).

The Qaidam basin has been characterized by endorheic drainage through most of its existence (Paleogene to recent), which resulted in the formation of a large continental lake (Chen and Bowler, 1986; Liu *et al*., 1998; Shi *et al*., 2001). The Pliocene and Quaternary fill of the Qaidam is exclusively terrestrial and comprises alluvial fan deposits, such as conglomerate and breccia disposed along basin margins. In contrast, the central sectors of the basin can be divided into:

— near-shore with mainly sand and siltstone,

— deep-water deposits, with many thin carbonate intercalations.

Various evaporitic minerals, for examples, sulphates and chlorides, formed during Pliocene to Quaternary regressive phases of lake development (Chen and Bowler, 1986; Lowenstein *et al*., 1989).

During the Pliocene to Quaternary, there has been a strong tectonic as well as climatic control of sedimentation. Generally the Pliocene to Quaternary are characterized by the driest climate of the Qaidam basin during Cenozoic time. The climatic shift towards arid condition has been related to uplift of the Tibetan Plateau which led to to strengthening of the monsoonal circulation (Wang *et al*., 1999 and reference therein). We will briefly discuss the main stages of basin history during these periods.

During the late Miocene to early Pliocene, the lake expanded to 200 km from north-west toward south-east. Towards the late Pliocene some of the lakes evolved to an evaporite formation stage. The 1000 m salt-bearing layers contain sulphate and chloride sequences around 200 m thick (Chen and Bowler, 1986), the total thickness of the Pliocene deposits reaching up to 6000 m. The enhanced aridity was due to uplift of the basin in the western region, associated with subsidence in the east, as well as regional cooling (Zhisheng *et al*., 2001).

From the late Pliocene to the Quaternary, during periods of tectonic deformation, anticlinal and synclinal structures were formed, resulting in segmentation of depositional environments (Song and Wang, 1993; Meyer *et al*., 1998). Within the synclines, sedimentation continued and produced thick lacustrine sequences 3000 to 4000 m (Liu *et al*., 1998; Shi *et al*., 2001; Yan *et al*., 2002). During the Quaternary, the Qaidam basin evolved as an intramontane basin controlled by western and northern winds, away from the influence of the monsoon. The arid periods alternated with short semi-arid conditions resulting in the formation of large shallow lakes and evaporites (Lowenstein *et al*., 1989; Phillips *et al*., 1993; Liu *et al*., 1998; Duan and Hu, 2001; Shi *et al*., 2001).

Between the beginning of the Quaternary and *ca*. 300 ka, there is no detailed information about the climatic evolution of the basin. In contrast much work has been done on deposits younger than 300 ka. At 302±56, 138±6 and 16.3±2.2 ka, U/Th ages indicate transitions from high to low lake level at the end of continental glacial maxima, the ages being mea-

sured on salt layers deposited in the western Qaidam basin. (Phillips *et al*., 1993). Stable isotope data on fluid inclusions trapped in evaporites from the central part of the basin indicate cold and wet periods at between 50 to 45, 42 to 34 and 28 to 19 ka. Lake level lowering and evaporite formation continued between 19 and 11 ka during a generally dry period. Lake levels rose again during late-glacial and post-glacial times, between 19 and 14 ka, but the age of this event may differ from site to site (Phillips *et al*., 1993; Yang *et al*., 1995). Generally, the Holocene is characterised by arid relatively warm climatic conditions.

Sulfate-rich brines occur in the western region of the basin, in contrast with those from the central part which are transitional between sulfate and chloride, with chloride brines predominating in the eastern sector (Chen and Bowler, 1986; Lowenstein *et al*., 1986). The thickness of the Pliocene to Quaternary evaporite-bearing strata decreases from west to east, because the evaporites started forming earlier in the western part.

The present climate represents the driest period during the last 40 ka, with mean annual precipitation of 25 mm in the centre of the basin and 100 mm along the border. Mean annual evaporation is ~3000 mm, while average temperature variations are from –10 to 20°C. The landscape is characterised by salt lakes, playas and aeolian landforms. Playas and salt lakes, as for example Yiliping and Quarhan, cover about one quarter of the total basin area.

METHODS

Mineralogical compositions were determined using a *Siemens D500* powder diffractometer at the Department of Mineralogy at the Landesmuseum Joanneum, Graz, Austria. The samples were prepared with a dental micro-drill and mounted on a glass plate. Microbeam analyses were performed at the Institute of Earth Sciences, using a *Jeol JSM-6310* scanning electron microscope equipped with ED- and WD-spectrometers.

Organic carbon content (TOC) was analysed by *LECO CS 300* combustion instrumentation and infrared detection at the Institute of Earth Science, University of Graz, Austria. The samples were weighed, treated with 2N HCL solution in order to dissolve carbonates, weighed again and than analysed for TOC.

Carbonate isotopic analyses were performed on whole-rock samples using an automatic Kiel II preparation line and a *Finnigan MAT Delta Plus* Mass Spectrometer at the Institute of Earth Sciences at the University of Graz, Austria. Reaction of calcite and dolomite with H_3PO_4 was done at 70EC. NBS-19 and an internal laboratory standard were analysed continuously for accuracy control (Bojar *et al*., 2001). Analytical precision is 0.1‰ for $\delta^{18}O$ and 0.06‰ for $\delta^{13}C$. All isotopic results are reported in permil units relativ to SMOW and PDB, respectively.

Sulphate isotopic analyses were done at the Institute of Geological Sciences, University of Wrocław. Sulphates were dissolved in an 18% HCl solution. The solution was filtered and $BaSO_4$ was precipitated, due to addition of 10% $BaCl_2$ solution. The precipitated $BaSO_4$ was rinsed with redistilled water, dried, weighed, powdered in an agate mortar, preheated at 550°C (2 minutes) and weighed again in order to calculate the concentration of sulphate (see Jędrysek, 2000).

For sulphur isotope analysis, 10 mg of $BaSO_4$ were mixed with 100 mg of V_2O_5 and 100 mg of pure quartz (Yanagisawa and Sakai, 1983). The mixture was placed at the bottom of quartz glass tubes together with preheated pure copper wire. The tube was attached to the vacuum preparation line and heated at 450°C for approx. 10 minutes to remove any volatile contaminants. Afterwards, the temperature was raised to 950°C and maintained for 25 minutes to complete the reaction. The obtained was frozen in a liquid nitrogen trap and then cryogenically cleaned using dry ice-ethanol mixture (Jędrysek *et al*., 2002). Alternatively, the SO_2 was obtained using $NaPO_3$ reagent (V_2O_5 yields the same results and both techniques have been used alternatively for calibration) as described by Hałas and Wołącewicz (1981). The sulphate was reacted under vacuum at 850°C with dry $NaPO_3$ and SO_3 were the gaseous products of this reaction. SO_3 was reduced to by passing the SO_3 over hot (approx. 700°C) pure copper.

For oxygen isotope analysis, it was necessary to obtain oxygen quantitatively as from $BaSO_4$. The CO_2 was prepared according to Mizutani and Rafter's (1973) technique; the sulphate was reacted with pure graphite at 1400°C under vacuum.

Sulphur and oxygen isotope analyses were carried out using a *Varian MAT CH7* mass spectrometer with a modified detection system. The $\delta^{18}O$ and $\delta^{34}S$ values are given in permil units with reference to SMOW and CDT international standards, respectively. The precision (1σ), obtained for complete analysis of replicate aliquots of standards and samples, was generally better than 0.1‰ for both sulphur and oxygen isotope analysis.

MICROFACIES, MINERALOGY AND STABLE ISOTOPIC COMPOSITION

Carbonate samples for stable isotope analysis from Quaternary strata are generally scarce and have mainly been collected from outcrops of the over Youshashan Anticline, Dafeng Shan, and Xiaoliangshan (Fig. 1). All stable isotope data from late Pliocene and Quaternary deposits are summarised in Table 1.

The Pliocene samples were collected from the southwestern side of the Youshashan Mountains and Ahati. Individual marl layers are 0.1 to 0.5 m thick. Their mineralogy consists of quartz, feldspar, calcite, ±muscovite, ±clinochlore, ±dolomite. The main carbonate is calcite. The $\delta^{18}O$ composition of carbonates vary between 22 to 26.1‰, the $\delta^{13}C$ between –3.8 to –1.1‰.

Generally the Quaternary samples show much higher values of the oxygen isotopic composition. Samples QA 297A-03, QA 298A-03 and QA 297A-01 were collected from shoreline deposits, near the basin border. The mineralogy consists of quartz, calcite, aragonite, ±muscovite, ±clinochlore, plagioclase. They show $\delta^{18}O$ values between 26.5 and 33.6‰ and $\delta^{13}C$ values between 0.1 and 4.6‰.

Table 1

Stable isotope results [‰] from Pliocene and Quarternary carbonates and sulphates from the Qaidam basin

Sample	^{13}C (carbonate PDB)	^{18}O (SMOW)	^{34}S (sulphate. CDT)	^{18}O (sulphate. SMOW)	Formation	Total organic carbon content [TOC %]	Age	Description
1	2	3	4	5	6	7	8	9
Dafeng Shan						0.06		
QA 260 A-03/1	–0.5	38.4	21.9	22.2	Qigequan		Quaternary	white crust, dolomite
2	–1.0	38.4			Qigequan			white crust, dolomite
3	–1.1	39.8			Qigequan			matrix, dolomite
4	–1.0	38.4			Qigequan			matrix, dolomite
QA 141C 1	–3.6	39.2	19.4	20.1	Qigequan	0.05	Quaternary	white oncoid, dolomite
2	–4.4	39.3			Qigequan			white oncoid, dolomite
3	–3.7	39.3			Qigequan			white oncoid, dolomite
4	–2.0	38.6			Qigequan			matrix, dolomite
5	–0.9	38.2			Qigequan			matrix, dolomite
6	–1.6	38.5			Qigequan			matrix, dolomite
7	–1.1	38.5			Qigequan			matrix, dolomite
8	–1.0	38.4			Qigequan			matrix, dolomite
QA 260B-03	–21.0	38.4	21.7	21.5	Qigequan	0.04	Quaternary	matrix, calcite/aragonite
QA 260C-03/1	–29.2	34.4			Qigequan	0.03	Quaternary	matrix, calcite/aragonite
	–30.3	35.7			Qigequan			matrix, calcite/aragonite
	–26.3	35.6			Qigequan			matrix, calcite/aragonite
	–26.3	35.6			Qigequan			matrix, calcite/aragonite
	–25.9	35.4			Qigequan			matrix, calcite/aragonite
	–30.5	35.5			Qigequan			matrix, calcite/aragonite
	–20.6	36.1			Qigequan			matrix, calcite/aragonite
	–23.9	36.0			Qigequan			matrix, calcite/aragonite
	–20.7	36.1			Qigequan			matrix, calcite/aragonite
QA 261B-03	–2.3	38.2	22.0	22.3	Qigequan		Quaternary	matrix, dolomite
	–2.4	38.3			Qigequan	0.04		matrix, dolomite

Tab.1 continued

1	2	3	4	5	6	7	8	9
Xiaoliangshan								
QA 298A-03	4.6	33.3			Qigequan		Quaternary	matrix, calcite/aragonite
	4.4	32.9			Qigequan			matrix, calcite/aragonite
QA 297A-03	0.1	31.2			Qigequan		Quaternary	matrix, calcite/aragonite
	3.4	33.6			Qigequan			matrix, calcite/aragonite
Qigequan Hills					Qigequan		Quaternary	matrix, calcite/aragonite
QA-297A-01	2.3	26.5						
Ahati								
QA-295B-03	0.7	26.1			Shizigou		Pliocene	matrix, calcite
E Youshashan								
QA-289A-03	–1.1	22.0			Shizigou		Pliocene	matrix, calcite
QA-294A-03	–2.4	22.2			Shizigou		Pliocene	matrix, calcite
QA-293A-03	–2.7	23.1			Shizigou		Pliocene	matrix, calcite

The approx. 25 m high exposure at Dafeng Shan contains, from the base to top, a succession of dolomite/celestine and calcite/aragonite layers, alternating with siltstones and fine sandstones (Fig. 2 A, B, C). The lower section is partly cut by meter-thick, discordant, NE-trending celestine veins. In Table 1 the samples are in stratigraphical order, from the bottom to the top. We described the microfacies according to Flügel (2004). For describing the carbonate rocks the classification of Folk (1959, 1962) modified after Strohmenger and Wirsing (1991) has been used.

Sample QA261B-03 contains dolomite, celestine, a few percent of halite and detrital quartz. The cement is composed of micritic dolomite and dolomitic ooids tens of microns across (Fig. 3A, B). The dolomite contains ~0.8 wt% iron. The celestine crystals are dispersed into the dolomitic matrix. The sample can be classified as a packed oomicrite (>50% ooids). The $\delta^{18}O$ and $\delta^{13}C$ of the dolomite is 38.2‰ and –2.3‰, respectively. For sample QA260C-03 (Fig. 4 A) the mineralogy consists of calcite, aragonite, ±barite, ±halite, and detrital quartz. The micritic cement consists of calcite, aragonite and barite (Fig. 4 B, C). The

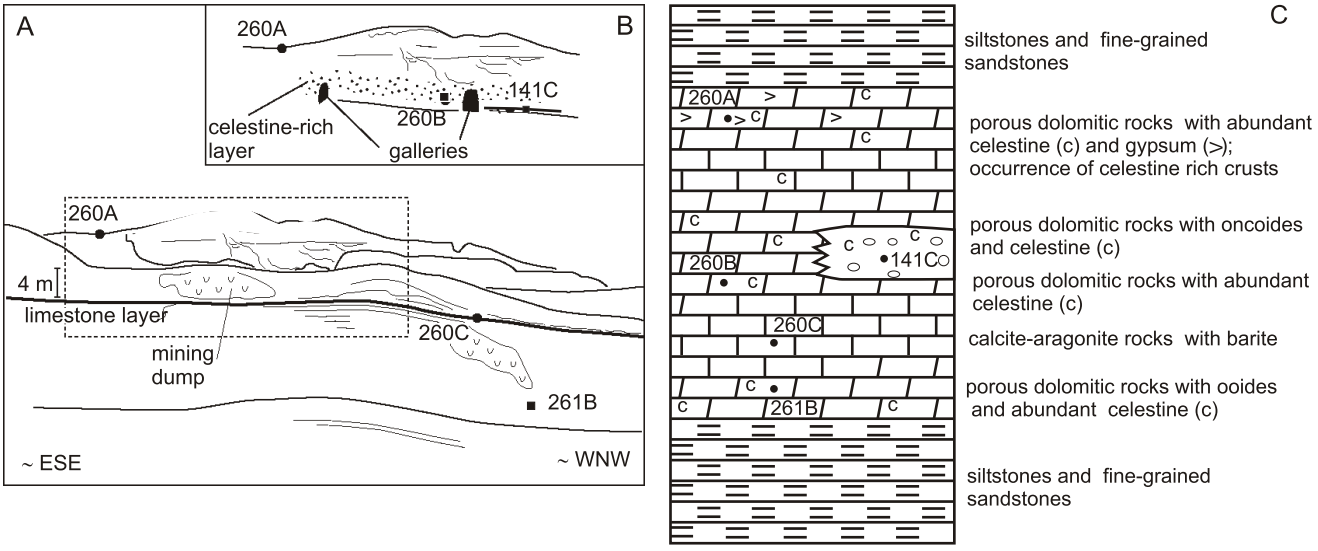

Fig. 2. Lithological section at Dafeng Shan mine showing the position of the Quaternary samples

A — overview from NNE, B — situation at mine entrance, C — lithological section (height — approximately 25 metres)

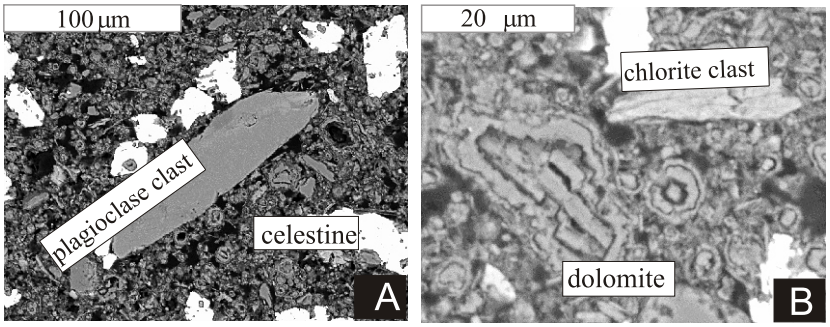

Fig. 3. QA 261B-03: A — BSE images: dispersed celestine crystals (white) within a dolomitic matrix; B — dolomitic oolites

Detrital clasts are sporadically found

barite locally contains up to 20% Sr (Fig. 4 D). Pyrite is concentrated within some layers. Characteristic of these layers is the presence of peloids tens of microns across, with a clotted structure. The peloids consist of calcite, aragonite, barite and pyrite (Fig. 4E–G). The sample can be characterized as a peloid-bearing micrite (between 1 to 10% peloids). An isotopic profile across the stratification of a hand specimen 15 cm across shows $\delta^{18}O$ values between 34.4 and 36.1‰ and a large variation in $\delta^{13}C$ values of between –20.7 and –30.5‰. Sample QA260B-03 contains dolomite and celestine, voids with celestine crystals being occasionally present (Fig. 5A, B). The dolomite shows $\delta^{18}O$ values of around +38.4‰ (SMOW), and $\delta^{13}C$ values around –21‰. Sample QA141C-01 contains mainly celestine and dolomite, subordinately halite and detrital quartz (a few percent). The sample contains also white, concentrically grown, ellipsoidal micrite oncoids filled with celestine, and dolomitic peloids showing a clotted structure (Fig. 6A–C). The sample can be classified as an oncomicrite. Voids filled with celestine crystals up to 2 mm across are also present. The micritic dolomite show $\delta^{18}O$ values around 38.4‰, and $\delta^{13}C$ values around –1.1‰. The oncoids have higher $\delta^{18}O$ values of +39.3‰ and lower $\delta^{13}C$ values of around –4‰. Sample QA260A-03 is characterised by a micritic matrix surrounding white crusts *ca*. 2 cm thick (Fig. 7 A). The cement is composed of dolomite, celestine and ±gypsum and clotted dolomitic peloids, the sample can be described as a sparse pelmicrite (Fig. 7 B, C). Thin halite layers are associated with the

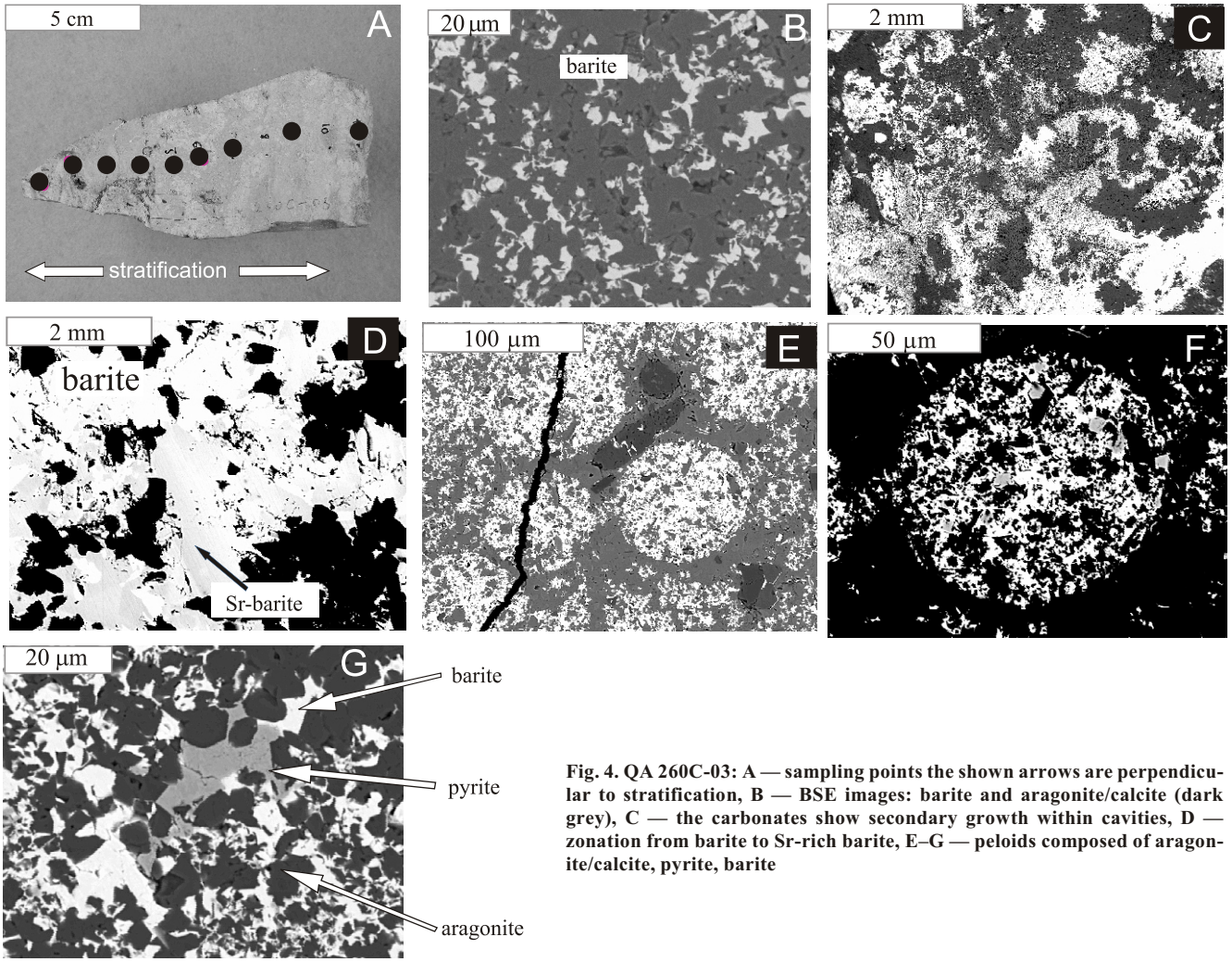

Fig. 4. QA 260C-03: A — sampling points the shown arrows are perpendicular to stratification, B — BSE images: barite and aragonite/calcite (dark grey), C — the carbonates show secondary growth within cavities, D — zonation from barite to Sr-rich barite, E–G — peloids composed of aragonite/calcite, pyrite, barite

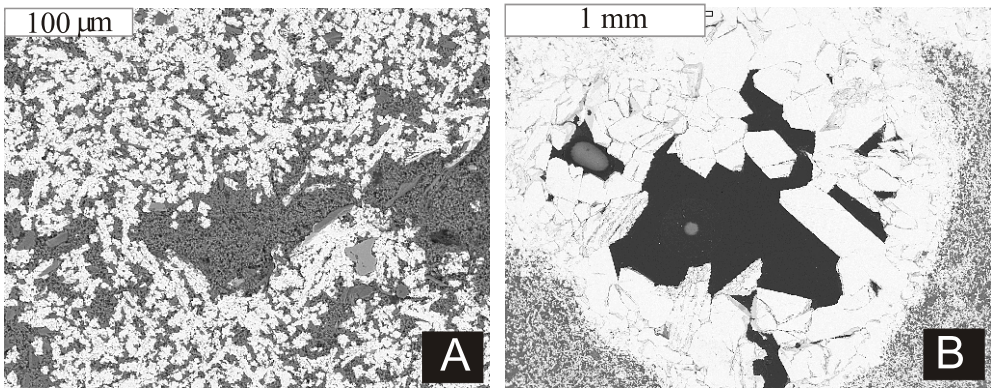

Fig. 5. QA 260B-03: A — BSE images: dolomite-celestine micrite, B — voids with celestine crystals

white crusts. Celestine crystals grow also in small voids. Both crusts and matrix show similar isotopic compositions, with $\delta^{18}O$ values ranging from 38.4‰ to 39.8 and $\delta^{13}C$ around –1‰.

For the sequence described at Dafeng Shan there is evidence that most of the observed microstructures are syn-sedimentary; for example, the preservation of *in situ* formed grains such as ooids, peloids and oncoids, the presence of celestine-halite crusts, the presence of open space pore showing local crystal growth, and the presence of aragonite. There is no evidence of deformation, re-crystallisation, pressure solution or secondary vein-fill within the thin sections.

For the Dafeng Shan exposure (Table 1), the $\delta^{18}O$ and $\delta^{34}S$ isotopic composition of celestine varies between –20.1 to 22.3‰ (SMOW) respectively from 19.4 to 22‰ (CDT). For all the samples from Dafeng Shan, TOC measurements have been made. The TOC shows little variation, with low values for all samples (Table 1).

The $\delta^{18}O$ values of Quaternary carbonates from the Dafeng Shan section vary between 34.4 and +39.8‰ (SMOW). These values are even higher than the ones reported for the calcites and dolomites associated with the saline deposits of the Pripyat Trough, Belarus (Maknach *et al*., 1994). In these the reported $\delta^{18}O$ values are up to +36.6‰, and have been considered the highest measured in continental carbonates. For marine carbonates developed under normal salinity conditions, the highest values reported until now are for siderites from Black Outer Ridge, for which values up to 39‰ (SMOW) are reported (Matsumoto, 1989). The $\delta^{13}C$ values show a large negative excursion from values of –2.3‰ in the lower part of the section (QA 261B-03) to values between –21 to –30‰ for QA 260C-03. In the upper part of the section, the matrix dolomite show values from –2 to –1‰ (QA 141C, QA 260A-03/1).

DISCUSSION AND CONCLUSIONS

The $\delta^{18}O$ values of lacustrine calcite cements that formed in near-surface meteoric phreatic conditions are dependent on water temperature and the $\delta^{18}O$ of the lake water. Since the late Pliocene as the lakes evolved as a closed system, with evaporation exceeding precipitation rates, we can consider the allogenic carbonate input negligible. For large shallow closed lakes it is usually assumed that water temperature reflects air temperature (Benson *et al*., 2002; Leng and Marshall, 2004). In contrast to

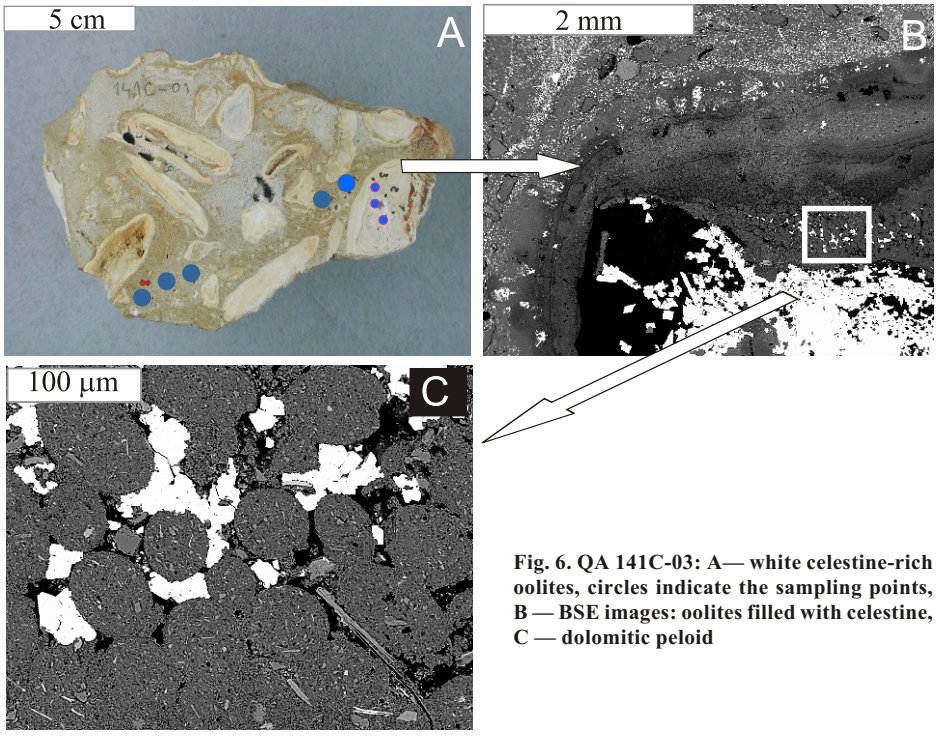

Fig. 6. QA 141C-03: A— white celestine-rich oolites, circles indicate the sampling points, B — BSE images: oolites filled with celestine, C — dolomitic peloid

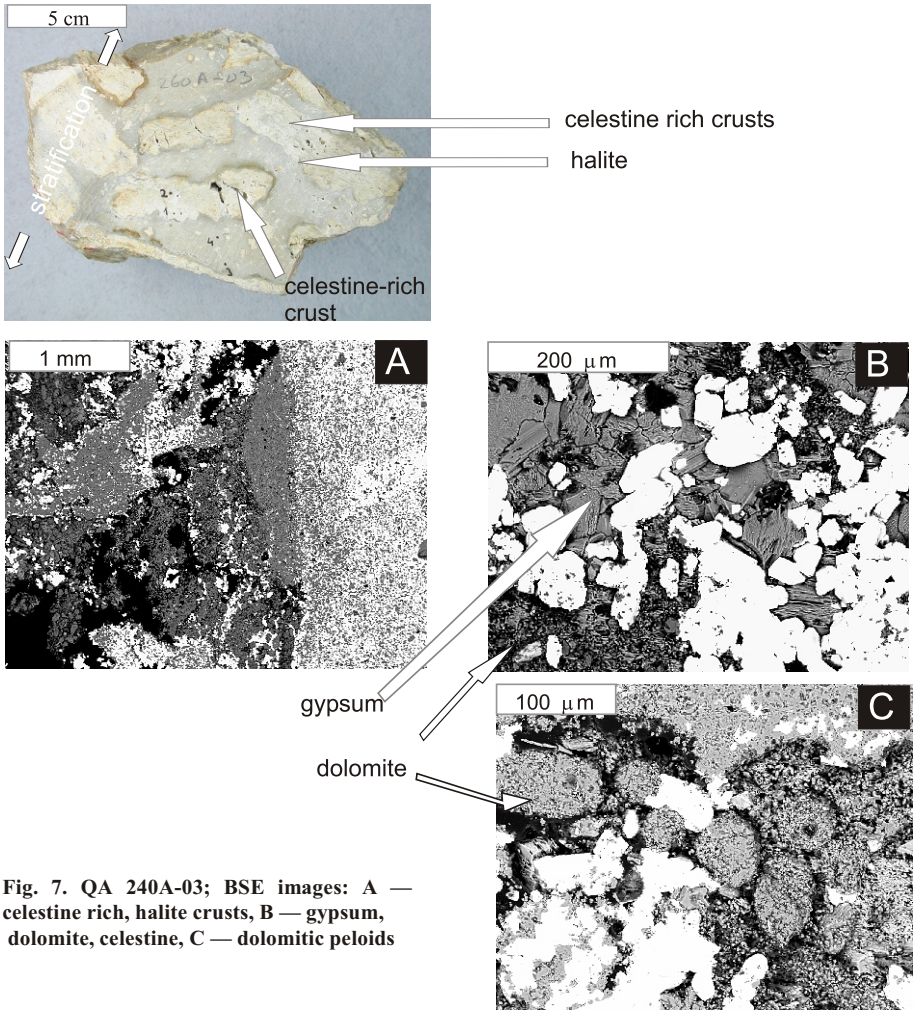

Fig. 7. QA 240A-03; BSE images: A — celestine rich, halite crusts, B — gypsum, dolomite, celestine, C — dolomitic peloids

the regions situated within a monsoon influence, the Qaidam basin during the Quaternary has shown low local air temperatures associated with high values of oxygen isotopic compositions of carbonates (Tian *et al*., 2003; He *et al*., 2004).

Isotopic data from the micritic cabonatic matrix indicate two different trends over the Pliocene and Quaternary (Table 1 and Fig. 8): a — a large positive $\delta^{18}O$ and a slight positive $\delta^{13}C$ shift between the Pliocene and Quaternary; b — during the Quaternary, for the Dafeng Shan outcrop, a large negative shift in the $\delta^{13}C$ values.

The large positive shift in $\delta^{18}O$ values between the Pliocene and Quaternary is interpreted as a climatic change from relatively humid conditions to cool, arid conditions. Such high aridity conditions and a closed lake environment were deduced for Quaternary strata of this region from other proxies such as, for instance the widespread salt-deposits and the pollen distribution (Chen and Bowler, 1986; Lowenstein *et al*., 1989; Xingzhen and Hongshun, 1993; Liu *et al*., 1998; Wang *et al*., 1999; Lehmkuhl and Haselein, 2000).

The presence of celestine and barite also indicates hypersaline conditions. Ba is less soluble than Sr by three and a half order of magnitude and, additionally, during precipitation from aqueous solution Ba is preferentially incorporated into the solid phase (Hanor, 2004). In order to leach Sr and precipitate celestine, highly saline fluids, with a significant concentration of dissolved sulfate and a high Sr/Ba ratio of the leached material should be available (Hanor, 2000). These fluids could penetrate into underlying sediments, leaching pre-existent carbonates or evaporites. Sr solubility decreases with temperature, therefore low-temperature fluids were required for transport. The extremely high ^{18}O compositions of dolomite also support a strongly evaporative, closed lake, where such high salinity fluids could develop. Microstructures, the presence of evaporitic minerals as well as the absence of lithoclasts support a low energy, hypersaline lacustrine environment for the formation of the sequence described at Dafeng Shan. There is increasing evidence about the *in situ* formation of particles as peloids, ooids and oncoids due to microbial activities in saline lakes (Flügel, 2004). The clotted structure of the peloids described points also towards a microbial origin for these grains

In the Qaidam basin, the average monthly temperatures vary between –10 and +20°C (Tian *et al*., 2003). As the lake was shallow, we can assume that the water temperature reflects the average monthly temperature, and that carbonates precipitated at temperatures between 0 and 20°C. For the assumed temperature range we can test if the measured isotopic composition of dolomites and aragonite/calcite indicate precipitation from a fluid with similar oxygen isotopic composition or not. We used for the calculations the fractionation factors of O`Neil *et al*. (1969) for calcite-water, Grossman and Ku (1986) for aragonite-water, and Matlhews and Kaltz (1977) for dolomite-water. The calculations show that for the assumed temperature range, the oxygen isotopic composition of dolomite is enriched by 3.2 to 4‰ with respect to pure calcite and enriched by 2.8 to 3.6‰ with respect to a mixture composed of 70% calcite and 30% aragonite. This mixture represents the mineralogy determined for sample QA260C-03. The mean value of the measured oxygen isotopic compositions for dolomite is 38.5‰ and that of calcite-aragonite mixture is 35.6‰. The difference between these values is 2.9‰, and in the range of calculated isotopic enrichment of dolomite with respect to a calcite-aragonite mixture. The measured isotopic compositions of matrix dolomite is quite constant and vary with 0.6‰ from 38.2 to 38.6‰ (see Table 1) and the isotopic compositions of calcite-aragonite vary with 0.7‰ from 35.4 to 36.1 (except one value). The isotopic enrichment of dolomite with respect to the calcite-aragon-

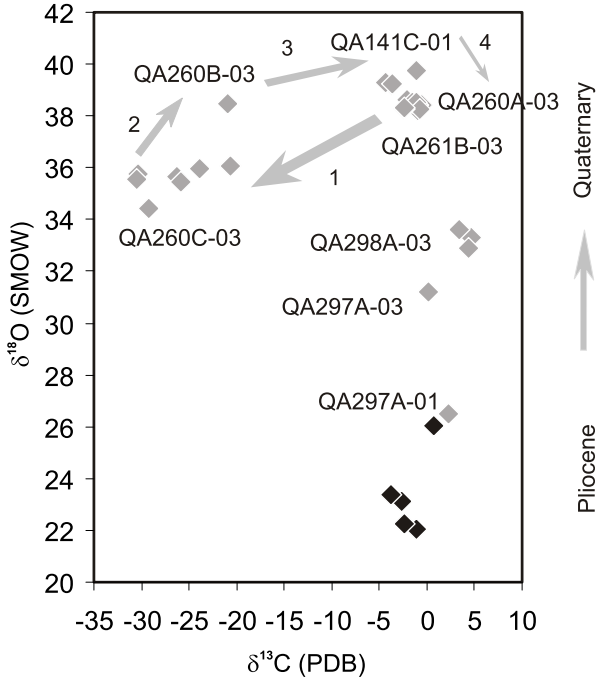

Fig. 8. Plot of $\delta^{18}O$ and $\delta^{13}C$ trends for Pliocene and Quaternary carbonates

The arrows indicate the relative stratigraphic position of the samples from Dafeng Shan from the bottom to the top of the outcrop

ite varies between 2.1 to 3.8‰ and it is in the range of calculated values. This fact suggests that the dolomite and calcite-aragonite precipitated from a fluid with similar oxygen isotopic composition. Thus the change in mineralogy from the Dafeng Shan, from dolomite-celestine to calcite-aragonite-barite, is more likely related to a change in water chemistry, for example, a drop in the sulphate concentration and increase in the carbonate concentration and/or change in redox condition as indicated by the presence of pyrite in the calcite-aragonite-barite sample QA260C-03.

The $\delta^{13}C$ isotopic composition of authigenic calcite is usually similar to that of ambient dissolved inorganic carbon (DIC). For a pH of between 6.4 and 10.3, HCO_3^- is the main DIC species (Clark and Fritz, 1997). We can expect, for such a hypersaline environment, rather alkaline conditions and the contribution of CO_3^{-2} species to the DIC. In this case the authigenic carbonates will reflect the $\delta^{13}C$ composition of dissolved HCO_3^- and CO_3^{-2} species. The calcite-bicarbonate fractionation is not temperature-dependent for carbon (Romanek *et al*., 1992), with the $\delta^{13}C$ isotopic value of calcite around 1‰ more positive. The fractionation factor between HCO_3^{-2} and HCO_3^- can be obtained by combining the equations of Mook *et al*. (1974) and Deines *et al*. (1974). The fractionation factor between these species is 0.4‰ and shows practically no variation with the temperature. By changing the distribution of the CO_3^{-2} and HCO_3^- species, the carbon isotopic composition of the carbonates will show a small variation of up to 0.4‰.

Usually the isotopic composition of DIC is controlled by: the isotopic composition of waters feeding the lake, photosynthesis/respiration of the aquatic plants and CO_2 exchange between atmosphere and lake water, oxidation of large amounts of organic materialerial. The Quaternary matrix carbonates show $\delta^{13}C$ values between –2 and 4.6‰, values which are higher than those of the Pliocene carbonates. As the lake evolved as a hydrological closed lake system during the Quaternary, the $\delta^{13}C$ values are interpreted to indicate different degrees of equilibration of the DIC with the atmospheric CO_2 (Talbot, 1990). For example, for atmospheric CO_2, which normally has values of –8‰, the $\delta^{13}C$ isotopic composition of DIC would have values around 2‰, similar to those measured for the Quaternary carbonates.

The large negative carbon isotopic excursion from the Dafeng Shan cannot be explained by the variation of one of the factors which usually control the DIC. Usually light ground waters in equilibrium with CO_2 gas at 20°C with $^{13}C_{CO2gas}$ of –23‰, have a $^{13}C_{DIC}$ of –15‰, which is further in isotopic equilibrium with a calcite characterized by a $^{13}C_{calcite}$ value of around –14.5‰ (Fritz and Fontes, 1997). Moreover as the TOC contents of the samples from Dafeng Shan are very low the presence of light CO_2 derived from oxidation of large amount of organic matter can be excluded. Only in highly organic shallow lakes, organic matter oxidation can lead to very low $^{13}C_{calcite}$ dropping to –19‰ (Eastwood *et al*., in press). Using the fractionation factor for carbon between: $CaCO_3$-CO_2 gas (Bottinga, 1968) and HCO_3^--CO_2 gas (Mook *et al*., 1974), we can calculate, from the lightest $^{13}C_{calcite}$ we measured, the $\delta^{13}C_{CO2gas}$ and the $^{13}C_{DIC}$ in isotopic equilibrium with this calcite. For temperatures between 0 and 20°C the calculated $\delta^{13}C_{CO2gas}$ values are between –45‰ and –41‰ and the $^{13}C_{DIC}$ are between –36 and –31‰, so far below the typical $^{13}C_{DIC}$ values of groundwaters.

There are also other mechanisms which may control the composition of lacustrine inorganic carbon DIC, such as the presence of CO_2 resulting from microbial, aerobic or anaerobic oxidation of methane. Bacterial oxidation of methane takes place either in the anoxic environment by sulfate-reducing bacteria when sulfate is available, or in anoxic environment through the activities of methane-oxidizing bacteria (Barker and Fritz, 1981; Sweeney, 1988; Whiticar, 1999). An excess of methane from deeper sources may reach the sediment-water interface, so in this case a combination of both oxidation processes may be possible. Bacterially produced methane is strongly depleted in ^{13}C, and shows ^{13}C values in the range of –50 to –110‰ (Whiticar, 1999). Thermogenically produced methane has a heavier compositions in the range of –20 to –50‰ (Sackett, 1978; Whiticar, 1999). In the region from where the samples come, the ^{13}C of known methane deposits range between –35 to –45‰ (Zhang *et al*., 2003), indicating a thermogenic origin. The isotopic composition of the carbonates with a methane-derived carbon source will be generally heavier than those of the methane itself because: a) during methane oxidation processes, the fractionation factor for carbon between CO_2 and CH_4 is positive and according to Whiticar (1999) between 30 and 5‰; b) carbon sources, other than methane, contain relatively more ^{13}C (Campbell *et al*., 2002; Peckmann and Thiel, 2004). For example, for a $^{13}C_{methane}$ of –45‰ there will result a CO_2 gas with ^{13}C of between –40‰ and –15‰ . The calculated carbon isotopic compositions of DIC and calcite in

equilibrium with this CO_2 gas at 20°C are: a $^{13}C_{DIC}$ between –31‰ and –6‰ and a $^{13}C_{calcite}$ between –30.5 and –5.5‰. At Dafeng Shan, the large negative shift in the carbon isotopic composition of carbonates, with variable values between –20 and –30‰, may be explained by participation of a light CO_2 resulting from methane oxidation. The isotopic composition of carbon from Dafeng Shan carbonates matches the isotopic composition of methane measured in the region, indicating rather bacterial oxidation of the thermogenically derived methane. According to our calculations, the oxidation of a methane with lighter compositions than these measured until now, and the presence of bacterial methane cannot be excluded, although no published data on the isotopic composition of such a methane are available. Pyrite, a common mineral in methane carbonates (Peckmann and Thiel, 2004) is also present in sample QA260A-03. It occurs as small pyritiferous carbonate nodules or as films within cavities with secondary carbonates. The presence of pyrite suggests anaerobic methane oxidation and sulfate reduction. If methane reached the sediment-water interface, we can also not exclude aerobic oxidation and liberation of a light CO_2 into the pool. The light CO_2 will also shift the carbon isotopic signature of primary carbonates to lower values. The microfabrics of QA260-03 show primary carbonates with upwardly-directed aggregation and secondary carbonates grown below carbonate crusts and within cavities. This fabric may be interpreted as supporting the presence of both aerobic and anaerobic methane oxidation. In this case, aggregation is associated with precipitation of carbonates from the lake water and the secondary carbonates formed during anaerobic oxidation of methane (Fig. 4C).

In non-marine evaporites, the stable isotope composition of sulphates reflects local sources and processes. As the basin is situated in the continental interior, in the rain shadow of the Himalayas, we can exclude the presence of marine aerosols as a potential source for sulphates. The basin has also a thick (averaging 8 km) continental sequence, so dissolution of pre-existing marine evaporites is not probable. Therefore we considered that for the Qaidam basin, the sulfates could be derived from dissolution of pre-existing continental evaporites and/or oxidation of sulfides from area surrounding the basin. The temperature dependence of sulfur isotope fractionation is low and similar among sulphate minerals. At low temperatures, isotopic exchange between dissolved sulphate and water has slow exchange rates (Chiba and Sakai, 1985). Accordingly, the sulfur and oxygen isotopic composition of celestine should reflect the composition of the dissolved sulphates, and not that of water.

The sulfur fractionation between sulfate minerals and aqueous sulfates is small (Holser and Kaplan, 1966; Sakai, 1968), therefore the sulfur isotopic composition will approximate to the isotopic composition of the parent fluid. The ^{34}S of the seawater sulfate is 1.65 less than that of the mineral (Thode and Monster, 1965), seawater sulfate having approx. 21‰ (CDT) (Rees *et al*., 1978; Longinelli, 1983). The ^{34}S isotopic composition of celestine from the Dafeng Shan varies between 19.4 to 21.9‰ (CDT) and it is by 3.3 to 0.7‰ lighter than the composition of the sulfates precipitated from seawater. The oxygen isotopic composition of celestine from Dafeng Shan varies between 20.1 to 22.3‰ (SMOW). The ^{18}O of the associated dissolved sulfate is 3.5‰ less than that of the mineral (Gonfiantini and Fontes, 1963; Lloyd, 1968), thus the isotopic composition of water sulfate varied between 16.6 and 18.8‰ (SMOW). These values are heavier than the present-day dissolved marine sulfate, which is approx. ~9.5‰ (Longinelli and Craig, 1967; Rafter and Mizutani, 1967; Longinelli, 1983) but they are in the range of isotopic compositions of sulfate ions from continental saline lakes and brines (Longinelli and Craig, 1967). The oxygen isotopic composition of sulphates measured at Dafeng Shan approach the value of dissolved atmospheric O_2 which is 24.2‰ (Dole *et al.*, 1954; Kroopnick and Craig, 1972) and suggests sulfur recycling via sulfide oxidation. One possible explanation for the stable isotope composition of sulfates from Dafeng Shan, characterized by slightly depleted sulphur and enriched oxygen isotopic composition in comparison to marine sulphate, would be oxidation of marine sulfides. It is known that sulfide oxidation mechanisms involve small sulfur isotope fractionations, while oxygen isotope fractionations range from 0 to –8.7‰ (Van Stempvoort and Krouse, 1994; Machel *et al*., 1995).

In conclusion, both $\delta^{13}C$ and $\delta^{18}O$ data, as well as the presence of evaporitic minerals, show a clear trend towards a dry climate during Quaternary times. In accordance with previous lithological and other environmental data, the oxygen isotopic compositions and mineralogy indicate that the coolest and driest conditions of the whole lifetime of the Qaidam basin occurred during the Quaternary. This may be correlated with a strong phase of surface uplift of both Himalayan and northern Tibet, and synchronously folding-induced segmentation of the basin. The lithological sequence from Dafeng Shan is interpreted to represent deposition of carbonate and evaporitic minerals during a dryer period alternating with wetter periods when fine siliciclastic minerals, as found at the bottom and top of the sequence, were deposited. A plausible explanation for the large negative shift of carbon isotopic composition found at Dafeng Shan is methane leakage from underlying natural gas and oil deposits. The oxygen isotopic composition of celestine minerals is heavier than that of the marine-derived sulfates, while the sulfur isotopic composition is slightly lighter than the composition of marine sulfates suggesting sulfur recycling via sulfide oxidation. The sulfides could be, for example, eroded from areas surrounding the basin

Acknowledgements. We acknowledge support for field work in the Qaidam basin by both NSF of China and Qinghai Oil Company. M.-O. Jędrysek, (Laboratory of Isotope Geology and Geoecology, Wrocław) is thanked for aid with the sulphate isotopic analyses. S. Hałas, (Lublin University) and K. Žak (Prague) are thanked for a helpful review. J. P. Smoot is thanked as well. For laboratory work financial support was provided by FWF Project 16258-N06.

REFERENCES

ALLÉGRE C. J., COURTILLOT C. V., TAPPONNIER P., HIRN A., MATTAUER M., COULON C., JAEGER, J. J., ACHACHE J., SCHÄRER U., MARCOUX J., BURG J. P., GIRARDEAU J., ARMIJO R., GARIEPY C., GOPREL C., LI T., XIAO X., CHANG C., LI G., LIN B., TENG J., WANG N., CHEN G., HAN T., WANG X., DEN W., SHENG H., CAO Y., ZHOU J., QIU H., BAO P., WANG S., WANG B., ZHOU Y. and XU R. (1984) — Structure and evolution of the Himalaya-Tibet orogenic belt. Nature, **307**: 17–22.

AN Z., KUTZBACH J. E., WARREN L. P. and PORTER S. C. (2001) — Evolution of Asian monsoon and phased uplift of the Himalaya-Tibetan plateau since late Miocene times. Nature, **411**: 62–66.

BARKER J. F. and FRITZ P. (1981) — Carbon isotope fractionation during microbial methane oxidation. Nature, **293**: 289–291.

BENSON L., KASHGARIAN M., RYE R., LUND S., PAILLET F., SMOOT J., KESTER C., MENSING S., MEKO D. and LINDSTRÖM S. (2002) — Holocene multidecadal and multicentenial droughts affecting Northern California and Nevada. Quater. Sc. Rev., **21**: 659–682.

BOJAR H.-P., BOJAR A.-V., MOGESSIE A., FRITZ H. and THALHAMMER O. A. R. (2001) — Evolution of veins and sub-economic ore at Strassegg, Paleozoic of Graz, Eastern Alps, Austria: evidence for local fluid transport during metamorphism. Chem. Geol., **175**: 757–777.

BOJAR A.-V., FRITZ H., NICOLESCU S., BREGAR M. and GUPTA R. P. (2005) — Quaternary exhumation mechanism of the Central Himalayan, evidence from fission track and (U-Th)/He data. Berichte des Institutes für Erdwissenschaften 8, Karl-Franzens-Universität Graz: 12–13.

BOTTINGA Y. (1969) — Calculation of fraction factors for carbon and oxygen in the system calcite-carbon dioxide-water. J. Phys. Chem., **72**: 800–808.

CAMPBELL K. A., FARMER J. D. and DES MARAIS (2002) — Ancient hydrocarbon seeps from the Mesozoic convergent margin of California: carbonate geochemistry, fluids and paleoenvironments. Geofluids, **2**: 63–94.

CLARK I. and FRITZ P. (1997) — Environmental isotopes in hydrogeology. Lewis Pub., New York.

CHEN K. and BOWLER J. M. (1986) — Late Pleistocene evolution of salt lakes in the Qaidam Basin. Qinghai Province, China. Palaeogeogr., Palaeoclimat., Palaeoecol., **54**: 87–104.

CHIBA H. and SAKAI H. (1985) — Oxygen isotopic exchange rate between dissolved sulfate and water at hydrothermal temperatures. Geochim. Cosmochim. Acta, **48**: 993–1000.

DEINES P., LANGMUIR D. and HARMON R. S. (1974) — Stable carbon isotope ratios and the existence of a gas phase in the evolution of carbonate groundwaters. Geochim. Cosmochim. Acta, **38**: 1147–1164.

DUAN Z. and HU W. (2001) — The accumulation of potash in a continental basin: the example of the Qarhan saline lake, Qaidam Basin, West China. Europ. J. Miner., **13**: 1223–1233.

FLÜGEL E. (2004) — Microfacies of carbonate rocks: analysis, interpretation and application. Springer Verlag.

FOLK R. L. (1959) — Practical classification of limestones. Am. Ass. Petrol. Geol. Bull., **43**: 1–38.

FOLK R. L. (1962) — Spectral subdivision of limestone types. In: Classification of Carbonate Rocks. A symposium (ed. W. E. Ham). Am. Ass. Petrol. Geol. Mem., **1**.

GONFIANTINI R. and FONTES J. CH. (1963) — Oxygen isotopic fractionation in the water of crystallisation of gypsum. Nature, **200**: 644–646.

GROSSMAN E. L. and KU T. L. (1986) — Oxygen and carbon isotope fractionation in biogenic aragonite; temperature effects. Chem. Geol., **59** (1): 59–74.

GUO Z. T., RUDDIMAN W. F., HAO Q. Z., WU H. B., QIAO Y. S., ZHU R. X., PENG S. Z., WEL J. J., YUAN B. Y. and LIU T. S. (2002) — Onset of Asian desertification by 22 Myr ago inferred from loess deposits in China. Nature, **416**: 159–163.

HAŁAS S. and WOŁĄCEWICZ W. (1981) — Direct extraction of sulphur dioxide from sulfates for isotopic analysis. Anal. Chem., **53**: 685–689.

HANOR J. S. (2000) — Barite-celestine geochemistry and environments of formation. In: Sulfate Minerals, Crystallography, Geochemistry and Environmental Significance (eds. C. N. Alpers, J. L. Jambor and D. K. Nordstrom). Rev. Miner. Geochem., **40**: 193–275.

HANOR J. S. (2004) — A model for the origin of large carbonate- and evaporite-hosted celestine ($SrSO_4$) deposits. J. Sediment. Res., **74**: 168–175.

HARRISON T. M., COPELAN P., KIDD W. S. and YIN A. (1992) — Raising Tibet. Science, **255**:1663–1670.

HE Y., THEAKSTONE W. H., ZHONGLIN Z., DIAN Z., TANDONG Y., TUO C., YONGPING S. and HONGXI P. (2004) — Asynchronous Holocene climatic change across China. Quater. Res., **61**: 52–63.

HODGES K. V. (2000) — Tectonics of the Himalaya and southern Tibet from two perspectives. Geol. Soc. Am. Bull., **112**: 324–350.

HOLSER W. T. and KAPLAN I. R. (1966) — Isotope geochemistry of sedimentary sulfates. Chem. Geol., **1**: 93–135.

JĘDRYSEK M.-O. (2000) — Oxygen and sulphur isotope dynamics in the of an urban precipitation. Water, Air Soil Poll., **117**: 15–25.

JĘDRYSEK M.-O., KAŁUŻNY A. and HOEFS J. (2002) — S and O isotope ratios in spruce needles as a tracer of atmospheric pollution. J. Geophys. Res. Atmosph., **107** (D18): ACH5-1–ACH5-12.

KAYAL J. R. (2001) — Micro earthquake activity in some parts of the Himalaya and the tectonic model. Tectonophysics, **339**: 331–351.

KROOPNICK P. and CRAIG H. (1972) — Atmospheric oxygen: isotope composition and solubility fractionation. Science, **175**: 54–55.

LEHMKUHL F. and HASELEIN F. (2000) — Quaternary paleoenvironmental change on the Tibetan Plateau and adjacent area (Western China and Western Mongolia). Quater. Internat., **65**–**66**: 121–145.

LENG M. and MARSHALL J. D. (2004) — Palaeoclimate interpretation of stable isotope data from lake sediment archives. Quater. Sc. Rev., **23** (7–8): 811–831.

LIU Z., WANG Y., CHEN Y., LI X. and LI Q. (1998) — Magnetostratigraphy and sedimentologically derived geochronology of the Quaternary lacustrine deposits of a 3000 m thick sequence in the central Qaidam basin, western China. Palaeogeogr., Palaeoclimat., Palaeoecol., **140**: 459–473.

LLOYD R. M. (1968) — Oxygen isotope behaviour in the sulfate-water system. J. Geophys. Res., **73**: 6099–6110.

LONGINELLI A. (1983) — Oxygen-18 and sulphur-34 in dissolved oceanic sulphate and phosphate. In: The Marine Environment (eds. P. Fritz and J. C. Fonts): 219–255. Handbook Environ. Isotope Geochem., Amsterdam, Elsevier.

LONGINELLI A. and CRAIG H. (1967) — Oxygen-18 variation in sulphate ions in sea water and saline lakes. Science, **146**: 56–59.

LOWENSTEIN T. K., SPENCER R. J. and ZHANG P. (1989) — Origin of ancient potash evaporites: clues from the modern nonmarine Qaidam Basin of Western China. Science, **245**: 1090–1092.

MACHEL H. G., KROUSE H. R. and SASSEN R. (1995) — Priducts and distinguishing criteria of bacterial and thermochemical sulfate reduction. App. Geochem., **110**: 373–389.

MAKNACH A., MIKHAJLOV N., SHIMANOVICH V. and KOSLOV I. (1994) — Carbon and oxygen isotopic composition of carbonates from saliferous deposits of the Prypiat Trough, Belarus. Sediment. Geol., **94**: 85–96.

MATLHEWS A. AND KATZ A. (1977) — Oxygen isotope fractionation during dolomitization of calcium carbonate. Geochim. Cosmochim. Acta, **41**: 1431–1438.

MATSUMOTO R. (1989) — Isotopically heavy oxygen-containing siderite derived from the decomposition of methane hydrate. Geology, **17**: 707–710.

MEYERHOFF A. A., KAMEN-KAYE M., CHIN C. and TANER I. (1991) — China- Stratigraphy, Paleogeography and Tectonics. Dordrecht, Boston, London. Kluwer Acad. Pub.

MEYER B., TAPPONNIER P., BOURJOT L., MÉTIVIER F., GAUDEMER Y., PELTZER G., SHUMIN G. and ZHITAI C. (1998) — Crustal thickening in Gansu-Qinghai, lithospheric mantle subduction, and oblique, strike-slip controlled growth of the Tibet plateau. Geophys. J. Int., **135**: 1–47.

MIZUTANI Y. and RAFTER T. A. (1973) — Isotopic behaviour of sulphate oxygen in the bacterial reduction of sulphate. Geochem. J., **6**: 183–191.

MOLNAR P. and TAPPONNIER P. (1975) — Cenozoic tectonics of Asia: effects of a continental collision. Science, **189**: 419–425.

MOLNAR P., ENGLAND P. and MARTIOD J. (1993) — Mantle dynamics, uplift of the Tibetan Plateau and the Indian monsoon development. Rev. Geophy., **34**: 357–396.

MOOK W. G., BOMMERSON J. C. and STAVERMAN W. H. (1974) — Carbon isotope fractionation between dissolved bicarbonate and gaseous carbon dioxide. Earth Planet. Sc. Lett., **22**: 169–176.

MURPHY M. A., YIN A., HARRISON T. M., DUERR S. B., CHEN Z., RYERSON F. J., KIDD W. S. F., WANG X. and ZHOU X. (1997) — Did the Indo-Asian collision alone create the Tibetan plateau? Geology, **8**: 719–722.

O`NEIL J. R., CLAYTON R. N. and MAYEDA T. K. (1969) — Oxygen isotope fractionation in divalent metal carbonates. J. Chem. Phys., **51**: 5547–5548.

PECKMANN J. and THIEL V. (2004) — Carbon cycling at ancient methane-seeps. Chem. Geol., **205**: 442–467.

PEIZHEN Z., MOLNAR P. and DOWNS W. R. (2001) — Increased sedimentation rates and grain sizes 2–4 My ago due to the influence of climate change on erosion rates. Nature, **410**: 891–897.

PHILLIPS F. M., ZREDA M. G., KU T., LUO S., HUANG Q., ELMORE D., KUBIK P. W. and Sharma P. (1993) — 230Th/234U dating of evaporite deposits from the western Qaidam Basin, China: implications for glacial-period dust export from central Asia. Geol. Soc. Am. Bull., **105**: 1606–1616.

PRELl W. L. and KUTZBACH J. E. (1992) — Sensitivity of the Indian monsoon to forcing parametrs and implications for its evolution. Nature, **360**: 647–652.

QIANG X. K., LI Z. X., POWELL C. M. and ZHENG H. B. (2001) — Magnetostratigraphic record of the Late Miocene onset of the East Asian monsoon, and Pliocene uplift of northern Tibet. Earth Planet. Sc. Lett., **187**: 83–93.

RAMSTEIN G., FLUTEAU F., BESSE J. and JOUSSAUME S. (1997) — Effect on orogeny, plate motion and land-sea distribution on Eurasian climate change over the past 30 million years. Nature, **386**: 788–795.

RAFTER T. A. and MIZUTANI Y. (1967) — Preliminary study of variations of oxygen and sulphur isotopes in natural sulphates. Nature, **216**: 1000–1002.

REES C. E., JUNKINS W. J. and MONSTER J. (1978) — The sulphur isotopic composition of ocean water sulphate. Geochim. Cosmochim. Acta, **42** (4): 377–382.

REPLUMAZ A. and TAPPONIER P. (2003) — Reconstruction of the deformed collision zone between India and Asia by backward motion of the lithospheric blocks. J. Geophys. Res., **108** (2285): 1-1-1-24.

ROMANEK C. S., GROSSMAN E. L. and MORSE J. W. (1992) — Carbon isotopic fractionation in synthetic aragonite and calcite: effects of temperature and precipitation rate. Geochim. Cosmochim. Acta, **56**: 419–430.

SACKETT W. M. (1978) — Carbon and hydrogen isotope effects during the thermocatalytic production of hydrocarbons in laboratory simulation experiments. Geochim. Cosmochim. Acta, **42**: 571–580.

SAKAI H. (1968) — Isotopic proprieties of sulfur compounds in hydrothermal processes. Geochem. J., **2**: 29–49.

SHI Y., YU G., LIU X., LI B. and YAO T. (2001) — Reconstruction of the 30-40 ka BP enhanced Indian monsoon climate based on geological records from the Tibetan Plateau. Palaeogeogr., Palaeoclimat., Palaeoecol., **169**: 69–83.

SONG T. and WANG X. (1993) — Structural styles and stratigraphic patterns of syndepositional faults in a contractional setting: examples from Qaidam Basin, Northwestern China. Am. Assoc. Petrol. Geol. Bull., **77**: 102–117.

SPICER R. A., HARRIS N. B. W., WIDDOWSON M., HERMAN A. B., GUO S., VALDES P. J., WOLFE J. A. and KELLEY S. (2003) — Constant elevation of southern Tibet over the past 15 million years. Nature, **421**: 622–624.

STROHMENGER C. and WIRSING G. (1991) — A proposed extension of Folk´s textural classification of carbonate rocks. Carbonat. Evaporit., **6**: 23–28.

SUN Z., FENG X., LI D., YANG F., QU Y. and WANG H. (1999) — Cenozoic Ostracoda and palaeoenvironments of the northeastern Tarim Basin, western China. Palaeogeogr., Palaeoclimat., Palaeoecol., **148**: 37–50.

SWEENEY R. E. (1988) — Petroleum-related hydrocarbon seepage in a recent North Sea sediment. Chem. Geol., **71**: 53–64.

TALBOT M. R. (1990) — A review of the palaeohydrological interpretation of carbon and oxygen isotopic ratios in primary lacustrine carbonates. Chem. Geol., **80**: 261–279.

THODE H. G. and MONSTER J. (1965) — Sulphur-isotope geochemistry of petroleum, evaporates, and ancient seas. Am. Assoc. Petrol. Geol. Mem., **4**: 367–377.

TIAN L., YAO T., SCHUSTER P. F., WHITE J. W. C., ICHIYANAGI K., PENDALL E., PU J. and YU W. (2003) — Oxygen-18 concentrations in recent precipitation and ice cores on Tibetan Plateau. J. Geophys. Res., **108** (9).

VAN STEEMPVORT D. R. and KROUSE H. R. (1994) — Controls of ^{18}O in sulfate: review of experimental data and application to specific environments. In: Environmental Geochemistry of Sulfide Oxidation, (eds. C. N. Alpers and D.W. BLOWES). ACS Symp. Ser. 550: 466–480.

WANG J., WANG Y. J., LIU Z. C., LI J. Q. and XI P. (1999) — Cenozoic environmental evolution of the Qaidam Basin and its implications for the uplift of the Tibetan Plateau and the drying of central Asia. Palaeogeogr., Palaeoclimat., Palaeoecol., **152**: 37–47.

WHITICAR M. J. (1999) — Carbon and hydrogen isotope systematics of bacterial formation and oxidation of methane. Chem. Geol., **161**: 291–314.

XIA W., ZHANG N., YUAN X., FAN L. and ZHANG B. (2001) — Cenozoic Qaidam basin, China: a stronger tectonic inversed, extensional rifted basin. Am. Ass. Petrol. Geol. Bull., **85**: 715–736.

XINGZHEN H. and HONGSHUN S. (1993) — Sedimentary characteristics and types of hydrocarbon source rocks in the Tertiary semiarid to arid lake basins of northwest China. Palaeogeogr., Palaeoclimat., Palaeoecol., **103**: 33–43.

YAN J. P., HINDERER M. and EINSELE G. (2002) — Geochemical evolution of closed-basin lakes: general model and application to Lakes Qinghai and Turkana. Sediment. Geol., **148**:105–122.

YANAGISAWA F. and SAKAI H. (1983) — Thermal decomposition of barium sulfate — vanadium pentaoxide — silica glass mixtures for preparation of sulfur dioxide in sulfur isotope ratio measurements. Anal. Chem., **55**: 985–987.

YANG W., SPENCER R. J., KROUSE H. R., LOWENSTEIN T. K. and CASAS E. (1995) — Stable isotopes of lake and fluid inclusion brines, Dabusun Lake, Qaidam basin, western China: hydrology and paleoclimatology in arid environments. Palaeogeogr., Palaeoclimat. Palaeoecol., **117**: 279–290.

YIN A. and NIE S. Y. (1996) — Phanerozoic palinspastic reconstruction of China and neighbouring areas. In: Tectonic Evolution of Asia (eds. A. Yin and T. M. Harrison): 442–485. Cambridge Univ. Press.

ZHANG X., HU Y., MA L., MENG Z., DUAN Y., ZHOU S. and PENG D. (2003) — Carbon isotope characteristics, origin and distribution of the natural gases from the Tertiary salty lacustrine facies in the West Depression region in the Qaidam Basin. Sc. China, Ser. D **46** (7): 694–707.

ZHISHENG A., KUTZBACH J. E., PRELL W. L. and PORTER S. C. (2001) — Evolution of the Asian monsoon and phased uplift of the Himalaya-Tibetan plateau since Late Miocene times. Nature, **411**: 62–66.

ZHOU D. and GRAHAM S. A. (1996) — Extrusion of the Altyn Tagh wedge: A kinematic model for the Altyn Tagh fault and palinspastic reconstruction of northern China. Geology, **24**: 427–430.